Załącznik 2 b

Self-presentation

1. Name:

Piotr Jan Wcisło

2. Education:

- 2011 – 2015, graduate studies in atomic and molecular physics at the Nicolaus Copernicus University in Toruń, Poland.
  PhD in Physics, title of thesis: ***Molecular collisions and shapes of optical resonances***
  Supervisor – Prof. Roman Ciuryło.

- 2005 – 2011, Undergraduate studies in Physics, Interdisciplinary Individual Studies in Mathematical and Natural Sciences (specialization in Optics and Atomic Physics) at the Jagiellonian University in Kraków, Poland.
  MSc in physics, title of thesis: ***Optical methods of magnetic field mapping***
  Supervisor – Dr hab. Szymon Pustelny.

- 2003 – 2005, Scholarship program for pre-university students skilled in the sciences, humanities and musics run by The Polish Children's Fund (Krajowy Fundusz na rzecz Dzieci). Under the program, participation in workshops and scientific camps in the field of solid state physics, quantum optics, and low temperature physics organized by the Polish Academy of Sciences.

3. Employment/research experience:

- Since 2017, Assistant professor at the **Nicolaus Copernicus University in Toruń**, Institute of Physics, Department of Atomic, Molecular and Optical Physics, Poland.

- 2018 – 2019, Postdoctoral Research Associate at **JILA (Joint Institute for Laboratory Astrophysics, University of Colorado & NIST)**, Boulder, USA, prof. Jun Ye group.

- 2015 – 2017, Research assistant at the **Nicolaus Copernicus University in Toruń**, Institute of Physics, Department of Atomic, Molecular and Optical Physics, Poland.

- 2016, Visiting Researcher (1 month) at the **Vrije Universiteit Amsterdam, Netherlands** (START program, Foundation for Polish Science). Collaboration with Prof. Wim Ubachs and Dr. Edcel Salumbides.

- Visiting Student Researcher at the **Harvard-Smithsonian Center for Astrophysics**, Cambridge, USA (6-month studies within the "Fulbright Junior Advanced Research Award 2014-15"). Supervisor: Dr. Lawrence S. Rothman.

Piotr Wcisło

4. The scientific achievement:

Title of the scientific achievement:

Series of publications:

"Practical and fundamental applications of accurate optical spectroscopy of atoms and molecules"

List of the publications accounting for the achievement:
(Detailed contributions are given in separate Appendices; statement of my contribution is given in Appendix 3, statements of all the other coauthors are in Appendix 4)

H1. **P. Wcisło**, I. E. Gordon, H. Tran, Y. Tan, S.-M. Hu, A. Campargue, S. Kassi, D. Romanini, C. Hill, R. V. Kochanov , L. S. Rothman,
The implementation of non-Voigt line profiles in the HITRAN database: H_2 case study,
J. Quant. Spectrosc. Radiat. Transf. 177, 75 (2016),
my contribution to the paper: 50%

H2. **P. Wcisło**, I. E. Gordon, C.-F. Cheng, S.-M. Hu, R. Ciuryło,
Collision-induced line-shape effects limiting the accuracy in Doppler-limited spectroscopy of H_2,
Phys. Rev. A 93, 022501 (2016),
my contribution to the paper: 70%

H3. **P. Wcisło**, F. Thibault, M. Zaborowski, S. Wójtewicz, A. Cygan, G. Kowzan, P. Masłowski, J. Komasa, M. Puchalski, K. Pachucki, R. Ciuryło, D. Lisak,
Accurate deuterium spectroscopy for fundamental studies,
J. Quant. Spectrosc. Radiat. Transf. 213, 41 (2018)
my contribution to the paper: 50%

H4. **P. Wcisło**, P. Morzyński, M. Bober, A. Cygan, D. Lisak, R. Ciuryło and M. Zawada,
Experimental constraint on dark matter detection with optical atomic clocks,
Nature Astronomy 1, 0009 (2016),
my contribution to the paper: 50%

H5. **P. Wcisło**, P. Ablewski, K. Beloy, S. Bilicki, M. Bober, R. Brown, R. Fasano, R. Ciuryło, H. Hachisu, T. Ido, J. Lodewyck, A. Ludlow, W. McGrew, P. Morzyński, D. Nicolodi, M. Schioppo, M. Sekido, R. Le Targat, P. Wolf, X. Zhang, B. Zjawin, M. Zawada,
First observation with global network of optical atomic clocks aimed for a dark matter detection,
Science Advances 4, eaau4869 (2018),
my contribution to the paper: 40%

4.1 Introduction and motivation of research

In recent decades a tremendous progress in optical and laser technologies has been observed. The revolution was triggered by the advent of laser sources, just five years after the famous experiment

by Gordon, Zeiger and Townes on amplification of microwave radiation by stimulated emission [Gordon1954, Gordon1955]. A number of incredible scientific and technological developments such as: electro- and acousto-optical systems, nonlinear optical components, polarization optics, laser diodes or fiber technology (just to mention a few) completely changed the perspective on the experimental studies on atoms and molecules. A crucial (Nobel-Prize-awarded) breakthrough was the invention of the optical frequency comb [Udem1999, Diddams2000] that allowed the time/frequency measurements to be linked with the optical domain, and hence opened a way to the construction of the optical atomic clocks [Ludlow2015] - the most precise instruments available to humanity. At the same time, the optical frequency combs together with other scientific and technological inventions like Pound-Drever-Hall stabilization scheme [Drever1983] or dielectric mirror coatings (enabling the cavity finesse to reach the 10^6 level) allowed construction of ultra-accurate cavity-enhanced spectrometers [Lin2015, Cygan2016] providing molecular spectra with signal to noise ratio exceeding 10^6 [Lin2015] and negligible apparatus function [Cygan2016], which is crucial for studying the structure of molecules [Polyansky2015, Wcisło2018], collisions between molecules and atoms [Jóźwiak2018] as well as for providing reference spectra for atmospheric studies [Ghysels2017]. These advancements opened a way to completely new research programs in atomic and molecular physics with applications to other fields. They also created a necessity to develop new theoretical and data-analysis approaches that allow the highly-accurate experimental data to be properly interpreted and associated systematic errors to be reduced. The submitted here achievement is in line with these research directions. It concerns the applications of the new spectroscopic methods (merging theory, experiment and data analysis) to the atmospheric studies as well as to fundamental studies on testing the quantum electrodynamics for molecules and searching for new physics beyond the standard model. In the first article [H1], a new approach to data-analysis of collisionally-perturbed spectra of molecular rovibrational transitions was developed and validated on highly-accurate experimental spectra; the goal is to use high-quality laser-spectroscopy reference data to reduce the systematic errors in spectroscopic studies of the atmospheres of Earth and other planets. Although this work is devoted to the particular case of hydrogen molecule, the methodology reported in Ref. [H1] is general and applicable to a wide class of atmosphere-relevant molecules. A crucial aspect of this work is that it introduced a new parameterization of the collisional effects perturbing molecular spectra; this representation was recently adopted [Gordon2017] in the most widely used spectroscopic database HITRAN (more than 10000 registered users). Articles [H2] and [H3] constitute continuation of work [H1], but instead of applications for atmospheric studies they focus on more fundamental physical aspects of ultra-accurate laser spectroscopy of molecular hydrogen. The collisional effects are calculated from first principles in a fully quantum way. A proper and reliable treatment of the collisional effects is used to reduce the systematic effects in our accurate measurements of the rovibrational transition. This not only allowed the quantum electrodynamics for molecules [Komasa2011] to be tested at high level of accuracy, but also can be applied in searches for new physics beyond the standard model (SM) [Ubachs2016] such as hypothetical long-range hadron-hadron interactions [Salumbides2013] or extra dimensions [Salumbides2015]. This research direction is continued in articles [H4] and [H5] where, instead of searching for new forces between known SM particles, a new method of searching for beyond-SM scalar fields that couples to the SM fields is proposed and experimentally implemented. This approach uses ultra-accurate optical spectroscopy of narrow atomic transitions; in Ref. [H4] the data recorded with optical atomic clocks operating in KL FAMO in Toruń is used, while Ref. [H5] benefits from a global network of optical atomic clocks (four clocks from USA, France, Poland and Japan). These results provide the stringent limits on the topological dark matter [Derevianko2014] and transient variations in the fine-structure constant.

4.2 Collisionally-perturbed spectra of molecular rovibrational transitions – atmospheric applications

The first paper within the submitted here achievement, Ref. [H1], is devoted to developing a new methods of analysis of molecular spectra from ultra-accurate laser spectroscopy. The molecular spectra measured at atmospheric conditions (i.e. conditions relevant for atmospheres of Earth and other planets and exoplanets) suffer from collisional perturbations. The most commonly used approach to analysis of spectroscopic data, based on a simple Voigt profile, is clearly insufficient and results in significant systematic errors in spectroscopic analysis of atmospheres [Smith1989] aiming on sub-percent accuracies [Miller2005]. The goal of this publication is to use highly-accurate molecular spectra from cavity-enhanced laser spectrometers to develop and validate new approach to molecular spectra analysis that can be applied to spectroscopic studies of atmospheres of Earth and other planets.

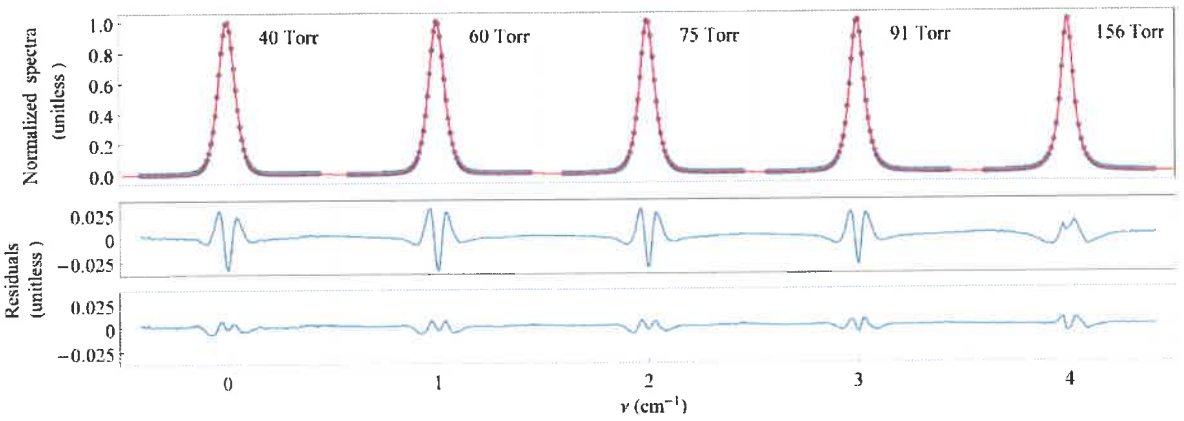

Fig. 1 The experimental spectra of self-perturbed H_2 3–0 S(1) line (blue points) and the HTP multispectrum fit (red curves). The middle and bottom panels are the residuals from the HTP multispectrum fit without and with the β correction, respectively.

In this analysis we used accurate experimental spectra of molecular hydrogen (relevant for gas giants atmospheres) collected with the highly accurate cavity ring-down spectroscopy (CRDS) [Campargue2012,Tan2014,Kassi2014] and optical feedback cavity-enhanced absorption spectroscopy (OF-CEAS) [Morville2005] in the laboratories in Grenoble (France) [Campargue2012,Kassi2014,Morville2005] and Hefei (China) [Tan2014]. Figure 1 (blue points in the top panel) shows the example of such spectra for the case of the second-overtone S(1) line at room temperature. A simple Voigt profile (i.e. convolution of Gaussian and Lorentzian) is completely inadequate since it does include any description of the velocity-changing collisions, which are responsible for such effects like Dicke narrowing (the residuals from the Voigt-profile fits are so large that we do not show them in Fig. 1). For the description including the velocity-changing collisions two extreme approaches may be adopted: a model originating from the interaction potential or purely phenomenological model. The first approach, in which the model of the molecular optical resonances is based on collisional kernels properly reproducing the kinetics of the H_2-H_2 collisions [Wcislo2014], such as speed-dependent billiard-ball profile (SDBBP), are computationally very expensive - this makes it impractical for direct atmospheric studies. For the second phenomenological approach, based on the simplest kernel (i.e. hard-collision kernel), there are existing computer algorithms which are computationally almost as efficient [Tran2013]

as the algorithms for the determination of the Voigt profile; we refer to the profile based on the hard-collision model and employing the quadratic approximation of the broadening and shift speed dependence as Hartmann-Tran profile (HTP). In the middle panel in Fig. 1, we show the residuals from the HTP multispectrum fit (the multispectrum fit is an approach in which the spectra are fitted to all the pressures simultaneously keeping the same values of the pressure-normalized collisional parameters for all of them – this allows the unphysical numerical correlations between different line-shape parameters to be reduced). From the middle panel in Fig. 1 it is clearly seen that the HTP does not account for the collisional effects properly since the amplitude of the residuals reaches 5 %. Such discrepancy may lead to systematic errors in atmospheric spectroscopic studies. The physical reason of this discrepancy is that the hard-collisions model (employed in HTP) constitute too crude approximation of the real collision kernel. Effectively, to first order, it manifests as nonlinear behavior of the frequency of the velocity-changing parameter, ν_{VC}, with pressure. To account for it we introduced a phenomenological function, β-correction function, rescaling the ν_{VC} parameter. As a reference, to determine the β-correction function, we used the speed-dependent billiard-ball model with experimentally evaluated speed dependence (SD_eBBP). SD_eBBP is based on much more physical collisional kernel (hard-sphere kernel), which was validated on molecular dynamic simulations [Wcisło2014]. In Figure 2, we show a difference between the HTP and SD_eBBP (red triangles) as a function of $\chi = \nu_{VC}/\Gamma_D$ parameter, where Γ_D is the Doppler width (in other words χ is a parameter which is proportional to pressure). It can be seen from Fig. 2 that at the intermediate pressure range when the Dicke narrowing is very pronounced (χ between 0.1 and 5) the relative peak-to-peak discrepancy can exceed 6 %. This is consistent with the amplitude of the residuals shown in the middle panel in Fig. 1. This discrepancy can be considerably reduced, almost without any further numerical expenses, by applying the developed here β-correction function. The β-correction is a function that nonlinearly (with pressure) rescale the rate of the velocity-changing collisions such as to adjust the simple HTP approach to the much more physical SD_eBBP model

$$\mathrm{SD}_e\mathrm{BBP}(\ldots,\nu_{VC},\ldots) \approx \mathrm{HTP}(\ldots,\beta(\chi)\nu_{VC},\ldots)$$

In Ref. [H1], we demonstrated that the β-correction function can be expressed by a simple analytical formula

$$\beta(\chi) = \theta(2.66-\chi)0.845\chi^{0.115} + \theta(-2.66+\chi)(1-0.38475\chi^{-2})$$

where θ is the Heaviside step function. In Figure 2, it is shown (see the black squares) that after applying the β-correction function to the HTP model the amplitude of the peak-to-peak residuals is reduced down to 2 %. In Figure 1 (see the bottom panel), it is shown that by employing the β-corrected HTP (instead of the usual HTP) in the multispectrum fit to the experimental data the residuals are decreased to the expected peak-to-peak 2 % level and (as shown in Ref. [H1]) the retrieved values of the line-shape parameters are much more physical. To sum up, in Ref. [H1] we developed a simple analytical correction to the HTP model and demonstrated that it allows one to reach a similar accuracy in the line-shape analysis as the much more sophisticated SD_eBBP model at much lower computational cost. This gives a tool for accurate atmospheric spectra analysis.

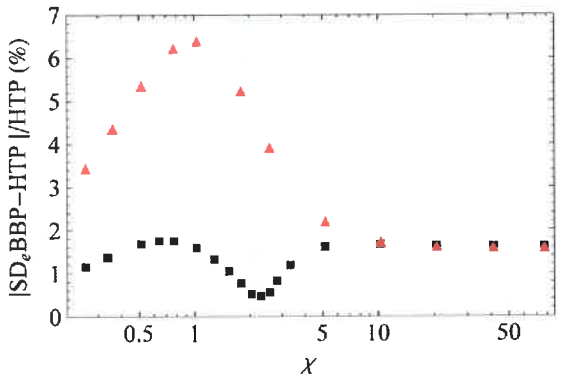

Fig. 2 The χ parameter dependence of the maximal relative difference between SDeBBP and HTP. The red triangles and black squares correspond to HTP without and with the β correction, respectively.

Another important aspect of the achievement reported in Ref. [H1] is a construction, for a given system (the H_2 molecule), of the first complete database of molecular lines, whose shapes go beyond the Voigt profile. These results are adopted in the most recent version [Gordon2017] of the HITRAN database. Not only the complete database for the H_2 molecule is included in the 2016 edition of HITRAN [Gordon2017] but also the developed in Ref. [H1] methodology and parametrization for handling the line-shape effects. Our approach splits the parametrization into four separate temperature ranges, which allows spectra representation at different temperature regimes, see Table 1. It should be emphasized that in Ref. [H1] we considered the H_2 case only, however the structure of the database supporting the HTP is more general and can be used for other molecules as well.

Table 1. HITRAN parametrization of Hartmann-Tran profile split into four temperature ranges. Detailed description and definitions of the these parameters are given in Ref. [H1]

Description of the parameters	The symbols of the parameters adopted in HITRAN (without specifying the profile, temperature range and perturber)	Notation[a] for HITRANonline [68] and HAPI [47] for different temperature ranges (in this example H_2(denoted as _self) is used as a perturber, but in general it can be replaced with any gas)			
		0 – 100 K T_{ref} = 50 K	100–200 K T_{ref} = 150 K	200–400 K T_{ref} = 296 K	> 400 K T_{ref} = 700 K
Half-width(speed-averaged)	$\gamma_0(T_{ref})$ (cm^{-1}/atm)	gamma_HT_0_self_50	gamma_HT_0_self_150	gamma_HT_0_self_296	gamma_HT_0_self_700
Temperature dependence of the half-width	n (dimensionless)	n_HT_self_50	n_HT_self_150	n_HT_self_296	n_HT_self_700
Speed dependence of the half-width	$\gamma_2(T_{ref})$ (cm^{-1}/atm)	gamma_HT_2_self_50	gamma_HT_2_self_150	gamma_HT_2_self_296	gamma_HT_2_self_700
Line shift (speed-averaged)	$\delta_0(T_{ref})$ (cm^{-1}atm)	delta_HT_0_self_50	delta_HT_0_self_150	delta_HT_0_self_296	delta_HT_0_self_700
Temperature dependence of the line shift	δ' (cm^{-1}/(atm K))	delta p HT self 50	deltap HT self 150	deltap HT self 296	deltap HT self 700
Speed dependence of the line shift	$\delta_2(T_{ref})$ (cm^{-1}/atm)	delta_HT_2_self_50	delta_HT_2_self_150	delta_HT_2_self_296	delta_HT_2_self_700
Frequency of velocity changing collisions	$\nu_{VC}(T_{ref})$ (cm^{-1}/atm)		nu_HT_self		
Temperature dependence of ν_{VC}	κ (dimensionless)		kappa_HT_self		
Correlation parameter	η (dimensionless)		eta_HT_self		

4.3 Collisionally-perturbed spectra of molecular rovibrational transitions – fundamental applications

Articles [H2] and [H3] constitute continuation of work [H1], but instead of applications for atmospheric studies they focus on more fundamental physical aspects of ultra-accurate laser spectroscopy of molecular hydrogen. The H_2 molecule, due to its simple structure (only two electrons and two protons), is a benchmark molecular system that allows the quantum electrodynamics for molecules [Komasa2011] to be tested at unprecedented level of accuracy. Furthermore, recently it was shown that the accurate spectroscopy of the rovibrational structure of H_2 can be used for the searches for new physics beyond the standard model (SM) [Ubachs2016] such as hypothetical long-range hadron-hadron interactions [Salumbides2013] or extra dimensions [Salumbides2015].

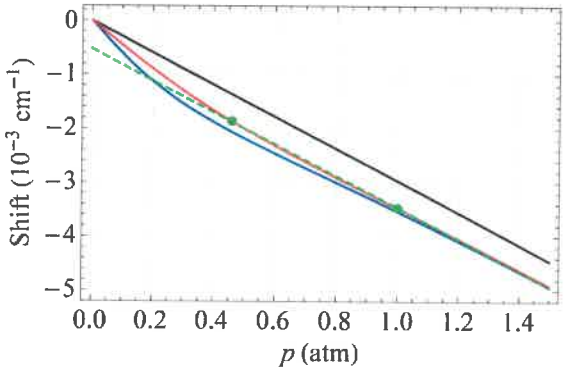

Fig. 3 Nonlinear behavior of the line position as a function of pressure for the case of the H_2 Q(1) fundamental line at T = 296 K (the blue and red lines correspond to the determinations of the line center from the maximum position and symmetric profile fits, respectively). The green dashed line shows the linear extrapolation from two shifts at p_2 = 1 atm and p_1 = 0.46 p_2. The extrapolation to zero pressure gives the systematic error of the unperturbed line position. The black line is the incorrect linear scaling assumed in the oversimplified description of the collisional effects.

In Ref. [H2] we demonstrated that the previously used experimental approach to the determination of the energy of the rovibrational transitions in H_2 [Cheng2012] considerably underestimates the systematic uncertainty due to oversimplified treatment of the collisional effects. The experiment from Ref. [Cheng2012] was based on ultra-accurate cavity-enhanced measurement at room temperature. We demonstrated that the effective line position (i.e. the energy of the transition) does not scale linearly with pressure, see Fig. 3, which has not been taken into account in the previous studies [Cheng2012]. We demonstrated that the reason of this nonlinear scaling was the speed dependence of the collisional shift, which is very pronounced for the case of molecular hydrogen and its effective influence is strongly correlated with the velocity-changing collisions [H2]. In Figure 4, we show how much this systematic effect influences the accuracy of the line position determined in Ref. [Cheng2012].

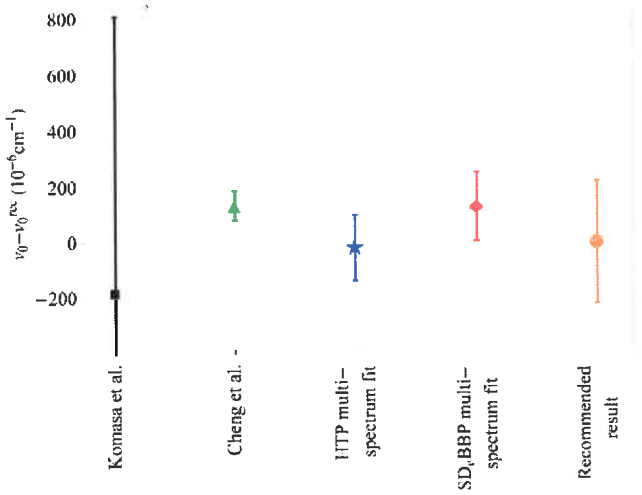

Fig. 4 Comparison of different approaches to determination of the H_2 (3-0) S(3) line position. Black square is the theoretical value calculated by Komasa et al. [Komasa2011]. The green triangle is the original determination from Ref. [Cheng2012]. The blue star and red diamond are our determinations with two different models when all the line-shape parameters were fitted. The orange circle is our ultimate determination with the fixed value of the speed dependence in the multispectrum fit - the determined value is 12 559.749 39 cm^{-1}, Ref. [H2].

In Ref. [H3], we applied the approach developed in Ref. [H2] to the case of the first-overtone transition in the D_2 isotopologue. The main result of this work is the most accurate determination of the energy of the D_2 2-0 S(2) transition; the total standard combined uncertainty is 401 kHz (which is more than nine significant digits). In Ref. [H3] we report:

- the results of our cavity-enhanced measurement of the shape of D_2 2-0 S(2) line (carried out in the National Laboratory FAMO in Toruń, Poland),
- the *ab initio* quantum-scattering calculations for the D_2-D_2 system for the states corresponding to the initial and final states of the D_2 2-0 S(2) transition,
- the spectra analysis based on one of the most advanced line-shape model and accurate determination of the D_2 2-0 S(2) transition energy,
- theoretical *ab initio* calculations of the rovibrational structure of the D_2 molecule that includes the relativistic and QED correction (this part was done by K. Pachucki, J. Komasa and M. Puchalski).

We measured the S(2) line from the 2-0 band of D_2 at four pressures (247.2, 471.3, 743.8 and 984.4 Torr) and at a temperature of 294.9 K, see the red points in Fig. 5. We used a deuterium sample having a purity of 99.96%. The spectra were collected with a frequency-stabilized cavity ring-down spectrometer (FS-CRDS) linked to an optical frequency comb (OFC) [Cygan2015]. The OFC was referenced to a primary time standard, the UTC(AOS) (Coordinated Universal Time from the Astro-Geodynamic Observatory in Borowiec, Poland). The length of the cavity was 74 cm, which corresponds to the free spectral range of 204 MHz. The cavity finesse was approximately 40,000. We averaged approximately 85 spectra at each pressure to achieve high signal-to-noise ratio (8500 at the highest pressure).

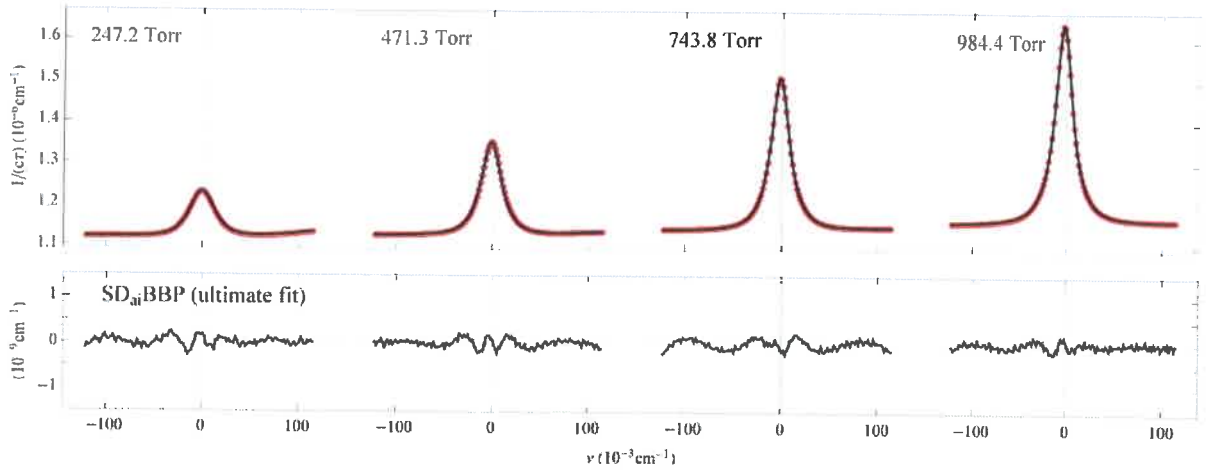

Fig. 5 Rovibrational 2-0 S(2) line of D_2 recorded with a frequency-stabilized cavity ring-down spectrometer (FS-CRDS) linked to an optical frequency comb (OFC). The top panel shows the experimental data (red points) and the fit (black lines) of the speed-dependent billiard-ball profile with *ab initio* speed dependence ($SD_{ai}BBP$). The residuals are shown in the bottom panel.

A crucial aspect of this work [H3] is to apply an approach to experimental spectra analysis that allow us to eliminate the systematic collisional errors [H2] related to the nonlinear scaling of the effective line position with pressure, see Fig. 3. For this purpose we performed *ab initio* calculations of the line-shape effects. First, we did quantum scattering calculations for the molecule-molecule system (i.e. the D_2-D_2 system) on a full six-dimensional potential energy surface [Hinde2008] for the both initial and final spectroscopic states and for all the rotational states of the perturbing D_2 molecule that are populated at room temperature (j = 0 to 5). By solving the close-coupling equations [Hutson1994] we obtained the energy-dependent scattering S-matrices, which are subsequently used to calculate the generalized spectroscopic cross sections [Monchick1986,Schaefer1992]

$$\sigma_\lambda^q(v_i j_i v_f j_f j_2; E_{kin}) ,$$

where E_{kin} is the kinetic energy of the collision, v_i and v_f (j_i and j_f) are the vibrational (rotational) quantum numbers of initial and final states of the considered transition, j_2 is the rotational state of the perturber. The q parameter is the tensor order of the transition (for the considered here quadrupole line q=2). We use the generalized spectroscopic cross sections to calculate the corresponding collisional integrals

$$\omega_\lambda^{s,s'}(q. j_2) = \langle v_r \rangle \int_0^\infty dx x^{(s+s'+2)/2} e^{-x} \sigma_\lambda^q(v_i j_i v_f j_f j_2; E_{kin} = x k_B T) ,$$

where

$$\langle v_r \rangle = \sqrt{8 k_B T/\pi \mu}$$

and μ and k_B are the reduced mass and Boltzmann constant, respectively. Finally, we employed the collisional integrals to calculate the first-order (usual broadening and shift parameters, Γ_0 and Δ_0) and higher-order (real and imaginary part of the frequency of the optical velocity-changing collisions, Re[ν_{opt}] and Im[ν_{opt}]) line-shape parameters

$$\Gamma_0 + i\Delta_0 = \frac{1}{2\pi c}\frac{p}{k_B T}\sum_{j_2} p_{j_2}\omega_0^{00}(q, j_2),$$

$$\nu_{\text{opt}} = \frac{1}{2\pi c}\frac{p}{k_B T}M_2\sum_{j_2} p_{j_2}\left[\frac{2}{3}\omega_1^{11}(q, j_2) - \omega_0^{00}(q, j_2)\right],$$

where p is pressure and p_{j_2} is the population of the perturber molecule in state j_2 at temperature T. For the case of molecular hydrogen the speed dependence of the Γ and Δ parameters is very pronounced and has to be incorporated in the line-shape model (the strong speed dependence of Δ is responsible for the nonlinear line-position scaling from Fig. 3 and associated with it systematic errors). We calculate the speed dependence of the Γ and Δ parameters, for a given speed of an active molecule, v, by averaging over the cross section over the relative speeds v_r [Pine1999]

$$\Gamma(v) + i\Delta(v) = \frac{1}{2\pi c}\frac{p}{k_B T}\sum_{j_2} p_{j_2}\frac{2}{\sqrt{\pi}\bar{v}_p v}\int_0^\infty dv_r v_r^2 e^{-\frac{v^2+v_r^2}{\bar{v}_p^2}}\sinh\left(\frac{2vv_r}{\bar{v}_p^2}\right)\sigma_0^q(v_i j_i v_f j_f j_2; v_r),$$

where $\bar{v}_p$ is the most probable speed of perturber. In Fig. 6 we show the speed dependence of the Γ and Δ calculated from *ab initio* cross sections for the case of the considered here S(2) line from the 2-0 band of D_2. The γ and δ parameters are the concentration-normalized counterparts of Γ and Δ.

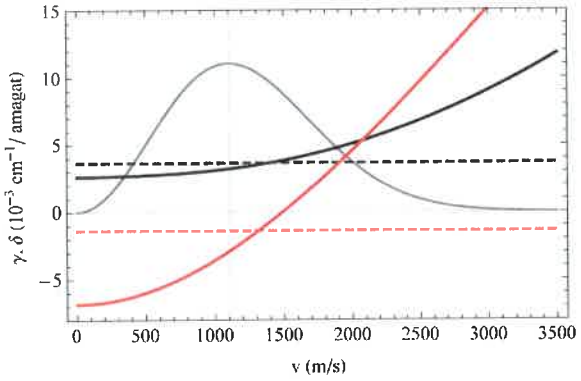

Fig. 6 Speed dependences of the broadening, γ (black solid), and shift, δ (red solid), parameters determined from our *ab initio* calculation for the deuterium S(2) 2-0 line at 294.9 K. The gray curve shows the Maxwellian speed distribution (arbitrary units) at the same temperature. The speed-averaged collisional broadening, γ_0, and shift, δ_0, are shown as the black and red dashed lines, respectively.

For the description of the velocity changing collisions we used the billiard-ball approximation of the collisional potential, which was validated on the molecular dynamics simulations [Wcislo2014]. Finally, the shapes of the rovibrational transitions

$$I(\omega) = \frac{1}{\pi}\text{Re}\int f(\omega, \vec{v})d^3\vec{v},$$

are calculated by solving the transport-relaxation equation

$$1 = -i(\omega - \omega_0 - \vec{k}\vec{v})h(\omega, \vec{v}) - \hat{S}^f h(\omega, \vec{v}),$$

where ω_0 is the position of the line and $\vec{k}$ is the wave vector of the probe laser. The function

$$f(\omega, \vec{v}) = f_m(\vec{v})h(\omega, \vec{v})$$

is a quantity proportional to the optical coherence associated with the transition under consideration. $f_m(\vec{v})$ is the Maxwell distribution of the active molecule velocities. The line-shape model emerging from the above description is called speed-dependent billiard-ball profile with *ab initio* speed dependence ($SD_{ai}BBP$).

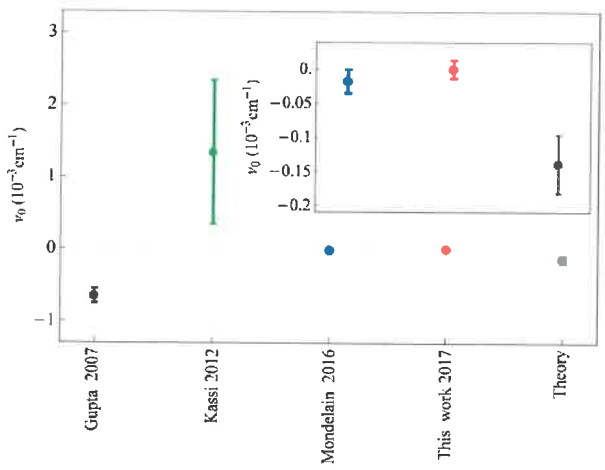

Fig. 7 Our experimental and theoretical determinations of the energy of the S(2) 2-0 line in D_2, red and gray dots respectively, compared with the previous experimental results: [Mondelain2016] (blue dot), [Gupta2007] (black dot) and [Kassi2012] (green dot). The inset shows the most recent values zoomed.

We employed the $SD_{ai}BBP$ to analyze our experimental spectra. The *ab initio* model of the collisions allowed us to considerably reduce the systematic errors (see Fig. 3) in determination of the energy of the rovibrational transition in D_2. In the bottom panel in Fig. 5, we show the residuals from the multispectrum fit with $SD_{ai}BBP$. The detailed discussion on the line-shape analysis and the related collisional effects are given in [H3]. In Table 2 we give the uncertainty budget. We reduced the dominating uncertainty contribution, i.e. the error originating from the collisional line-shape effects, down to 357 kHz, which allowed us to achieve the final standard combined uncertainty of 401 kHz. In Figure 7, we show comparison of the previous determinations. The accuracy of 401 kHz corresponds to 13×10^{-6} cm^{-1}. This allows the relativistic, QED and finite nuclear size corrections to be experimentally validated, see Table 3. **It should be emphasized that the 3.4 σ discrepancy between our experimental and theoretical values of the line position reported in [H3] was recently demonstrated to originate from errors in nonadiabatic relativistic corrections to the transition energy [Czachorowski2018]. The recent calculations [Czachorowski2018] revealed an agreement, within the declared uncertainties, between our experimental determination and *ab initio* calculations [Czachorowski2018].** Beyond the tests of the QED and relativistic corrections, the accurate measurements of the transition energies in the simplest molecule, i.e. molecular hydrogen, are used for searching for new physics beyond the standard model (SM) [Ubachs2016] such as hypothetical long-range hadron-hadron interactions [Salumbides2013] or extra dimensions [Salumbides2015].

Table 2. Contributions to the budget of standard uncertainties for our measurement of the frequency of the S(2) 2-0 transition in D_2, ν_0 = 187 104 300.038 (401) MHz.

Uncertainty source (type)	$u(\nu_0)$ / kHz
1) Statistics, 1σ (A)	132
2) Optical frequency comb (A+B)	< 1
3) Line-shape analysis (B)	357
4) Instrumental systematic shift (B)	47
5) Relativistic asymmetry (B)	< 3
6) Pressure gauge nonlinearity (B)	< 1
7) Etalons (B)	59
8) Temperature instability (A+B)	100
Standard combined uncertainty	**401**

Table 3. Different contributions to the energy of the S(2) 2-0 transition in D_2 determined from *ab initio* calculation. E(2), E(3), E(4), and E(5) are calculated in the Born-Oppenheimer (BO) approximation. The uncertainties due to nonadiabatic corrections are denoted by $()_{na}$. The other uncertainties are due to approximate numerical evaluation. EFS is the finite nuclear size correction. The last row is the combined value of these two experimental energies.

Contribution	cm^{-1}
$E^{(0)}$ (nonrelativistic)	6241.120920(1)
$E^{(2)}$ (α^2 relativistic)	$0.040057(20)_{na}$
$E^{(3)}$ (α^3 QED)	$-0.03315(3)(2)_{na}$
$E^{(4)}$ (α^4 QED)	−0.000299
$E^{(5)}$ (α^5 QED)	0.000019(10)
E_{FS}	−0.000032
Total theor.	**6241.127515(42)**
Expt.[a]	6241.127637(17)
Expt.[b]	6241.127655(13)
Combined expt.	**6241.127647(11)**

[a] Ref. [Mondelain2016].
[b] This work.

4.4 Spectroscopy of ultra-narrow atomic electronic transitions – fundamental applications

In papers [H4] and [H5], we continue the work from Refs. [H2] and [H3] (whose ultimate goal are searches for the new hypothetical long-range hadron-hadron interactions or extra dimensions), but instead of focusing on new interactions between the standard-model (SM) particles, in Refs. [H4] and [H5] we search for SM fields interactions with some new hypothetical scalar fields [Derevianko2014] that could explain the dark-matter puzzle. Similarly to Refs. [H1-H3] we benefit here from the recent advancements in ultra-accurate laser spectroscopy. However, instead of using molecules, in Refs. [H4] and [H5] we use ultra-narrow optical transition in cold atoms.

The objects we are aiming on are dark-matter topological defects in the scalar fields, ϕ, (with suitable self-potential) that could be produced in the early universe phase transitions [Derevianko2014, Vilenkin1985]. It was demonstrated that if such new hypothetical field couples to the SM field then, to first order, the QED Lagrangian (which governs the atomic physics) has the

same form as the original QED Lagrangian without such coupling, but the values of the fundamental constants would be perturbed. In Refs. [H4] and [H5] we focus on the coupling between the hypothetical scalar field with the electromagnetic field, which would be manifested as a variation in the fine-structure constant, α. We consider a coupling term in the Lagrangian which is quadratic in ϕ – the energy scale of this coupling, Λ_α, inversely quantify the strength of the topological defect interaction with electromagnetic field.

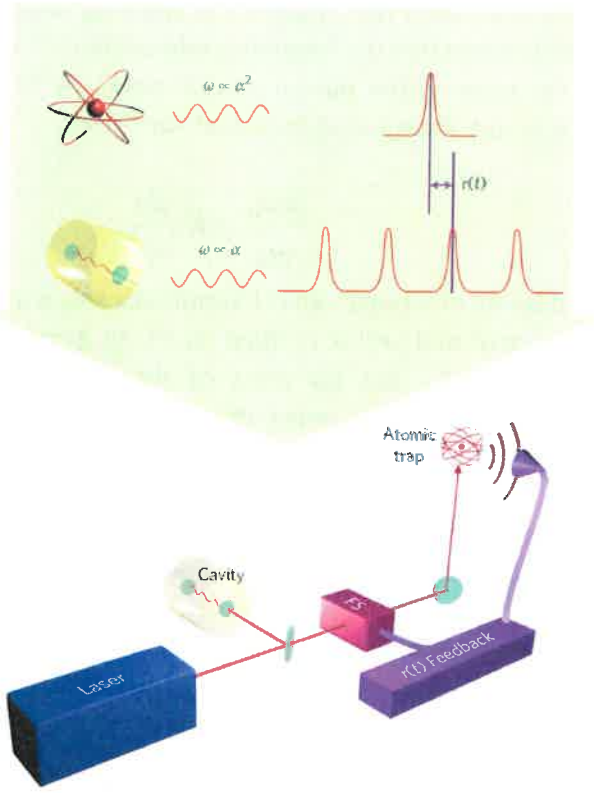

Fig. 8 Sensitivity of an optical atomic clock to topological dark matter (DM). When the clock traverses through a DM topological defect, DM will perturb the values of certain standard model (SM) parameters, hence, we may expect a transient variation in the fine-structure constant α. This will shift the frequency of the electronic clock transition and the frequency of the chosen cavity mode. Different sensitivities of the atoms and cavity to α variations makes a single optical atomic clock sensitive to hypothetical DM objects.

In Ref. [4] we demonstrated that a single optical atomic clock is sensitive to the variations in α and we used it to determine, for the first time with optical atomic clocks, the constraint on the coupling of the topological defect dark matter with the electromagnetic field. Our approach is shown in Fig. 8. We benefit from the fact that every optical atomic clock is equipped with two independent frequency references, i.e., cold atoms (their narrow electronic transition) and optical cavity. To show that the clock is sensitive to α variations, it has to be shown that the sensitivities to α variations of the two references are different. To show this, we analyze the electronic part of the Schrödinger equation (in the Born–Oppenheimer approximation), for a system composed of n electrons and m nuclei

$$\left(-\frac{\hbar^2}{2m_e}\sum_{i=1}^{n}\nabla_{r_i}^2-\alpha\hbar c\sum_{i,j=1}^{n,m}\frac{Z_j}{r_{ji}}+\frac{1}{2}\alpha\hbar c\sum_{\substack{i,k=1\\ i\neq k}}^{n,n}\frac{1}{r_{ik}}\right)\psi=E\psi,$$

where m_e is the mass of electron, Z_j is the number of protons in the j^{th} nucleus, $r_{ji} = |R_j - r_i|$ and $r_{ik} = |r_i - r_k|$. R_j and r_i are the coordinates of the j^{th} nucleus and the i^{th} electron, respectively. The entire α-dependence originates from the transformation of the above equation to its dimensionless form: $\epsilon = E/E_h$ and $x_i = r_i/a_0$, $x_{ji} = r_{ji}/a_0$ and $x_{ik} = r_{ik}/a_0$, with $E_h = \alpha^2 m_e c^2$ and $a_0 = \hbar/(m_e \alpha c)$. It is straightforward to see from this transformation that, in the SI units, the energies scales as $E \propto \alpha^2$ (therefore also the frequency of the atomic transitions scale as $\omega^{at} \propto \alpha^2$) and linear dimensions as $\propto \alpha^{-1}$. The $\propto \alpha^{-1}$ scaling of linear dimensions concerns also the solid-states spacers that set the length of optical cavities, hence the frequency of the longitudinal modes of the cavity scales as $\omega^{cav} \propto \alpha^1$. This analysis shows that the frequency references (ω^{cav} and ω^{at}) have different sensitivity to α variations. For most of the optical atomic clocks $\omega^{cav} \approx \omega^{at}$ (we denote the common approximated value as ω_0). If we define $d\omega_0 = d(\omega^{at} - \omega^{cav})$ then

$$\frac{d\omega_0}{\omega_0} = K_\alpha \frac{d\alpha}{\alpha},$$

where K_α is the sensitivity of a single optical atomic clock to α variations. It is straightforward to show that when $\omega^{at} \propto \alpha^2$ and $\omega^{cav} \propto \alpha^1$ then $K_\alpha = 1$. In general, one should also consider the relativistic corrections to K_α, but for most of the atomic species it is negligible. In our measurements we used Sr atoms for which the corrected value is $K_\alpha = 1.06$ (for heavier elements the correction can be larger, but still at the order of unity; for instance for mercury $K_\alpha = 1.8$).

For the measurement reported in Ref. [H4] we used two collocated optical-lattice clocks with neutral ^{88}Sr atoms [Bober2015,Morzyński2015] operating in National Laboratory FAMO in Toruń, Poland. We recorded the 12-hours-long readouts simultaneously with the two clocks operating in the synchronous mode (the interrogation of atoms was synchronized in every clock cycle). To analyze the readouts we used the concept of the cross-correlation function

$$(r_1 * r_2)(\Delta t) = \frac{1}{t_2 - t_1} \int_{t_1}^{t_2} r_1(t) r_2(t + \Delta t) dt,$$

where $r_1(t)$ and $r_2(t)$ are the readouts from the first and second clock, respectively (by readout, we mean the $\omega^{at} - \omega^{cav}$ difference), t_1 and t_2 are the beginning and end of the cross correlated periods. The constraint on the transient variation of α can be determined from the amplitude of the readouts cross-correlation, A_0,

$$\frac{\delta\alpha}{\alpha} < \frac{1}{K_\alpha} \frac{\sqrt{A_0/\eta_T}}{\omega_0},$$

where η_T is the is the ratio of the overall dark-matter signal duration to the length of the cross-correlated signals. We demonstrated [H4] that this limit can be directly translated into the constraint on the strength of the dark matter coupling to the standard-model electromagnetic filed

$$\Lambda_\alpha > d^{1/2} \sqrt{\sqrt{\frac{\eta_T}{A_0}} \rho_{\mathrm{TDM}} \hbar c K_\alpha \mathcal{T} v \omega_0},$$

where d is a thickness of the topological defect, ρ_{TDM} is the mean DM energy density, $\mathcal{T}$ is the time between encounters with topological defects, and v is the relative speed of the defects. In Figure 9, we show the constraint on Λ_α determined with our measurement, see the solid green line. It not

only exceeds the previous limits by several orders of magnitude, but also reaches the constraint achievable with the constellation of GPS clocks [Derevianko2014], despite that the analysis from Ref. [Derevianko2014] assumes more optimistic condition of $\mathcal{T}$ = 1 yr.

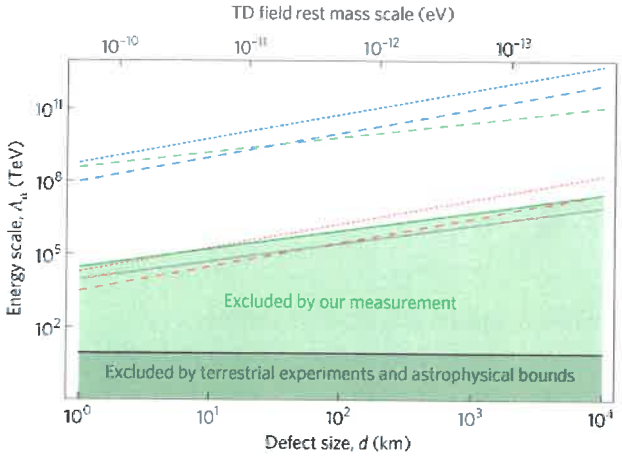

Fig. 9 Constraint on the strength of DM-SM coupling. The grey and green lines are the constraints inferred from our measurement by cross-correlating the readouts in their entirety and by cross-correlating only their small portion. The dashed blue and red lines are taken directly from Ref. [Derevianko2014]. They represent limits on the experimental constraints that could be achieved with a trans-continental network of Sr optical-lattice clocks (blue) and a GPS constellation (red). However, these limits turned out to be underestimated. The dotted blue and red lines are the corrected limits. The dashed green line represents the constraints achievable using our approach under the same conditions used in Ref. [Derevianko2014].

One of the major advantages of our method [H4] is that, in contrast to the original proposal [Derevianko2014], it is not limited by the need for a phase-noise-compensated optical fiber link, which is a crucial feature when a global Earth-scale network is considered. It is so, because in our approach the optical signals are compared locally and independently in every optical atomic clock. It, not only, makes our method much simpler to be implemented at global scale, but also make our approach completely immune to the residual noise present in any (even a phase-noise-compensated) optical fiber link [Calonico2015]. We benefit from this feature in Ref. [H5]. This approach allowed us to form the first Earth-scale network of optical atomic clocks aimed on the searches of topological dark matter and other effects related to transient variations in α. In Figure 10, we show the structure of our network. In its early stage, it is composed of four laboratories from three continents:

1. NIST, Boulder, CO, USA [Hinkley2013,Schioppo2016], ^{171}Yb optical atomic clock,
2. LNE-SYRTE, Paris, France [Targat2013,Lodewyck2016], ^{87}Sr optical atomic clock,
3. KL FAMO, Torun, Poland [Morzyński2015,Bober2015], ^{88}Sr optical atomic clock,
4. NICT, Tokyo, Japan [Hachisu2015, Hachisu2018], ^{87}Sr optical atomic clock.

The measurements were performed from 9 January 2015 to 17 December 2015 (11, 24, 42 and 54 days in NIST, LNE-SYRTE, KL FAMO and NICT laboratories, respectively). Together the laboratories collected data for 114 days.

Fig. 10 Global network of optical-atomic-clock sensors.

In our topological defect searches based on the global network [H5] we used the longest consecutive overlapping records for each pair of clocks. Their lengths are 3336 s for the NIST and LNE-SYRTE, and 13533 s for the LNE-SYRTE and KL FAMO cross-correlations. The new constraint on the strength of DM-SM coupling, i.e. the energy scale Λ_γ, is shown in Fig. 11, see the red line (the Λ_γ parameter is the same as Λ_α from Fig. 9). Thanks to employing the state of the art optical atomic clocks in the network, and thanks to the fact that the cross-correlated clocks were distant (and hence did not suffer from common noise, which was the case in the measurement from Ref. [H4]) the new constraint from Fig. 11 [H5] is about order of magnitude stronger than the previous one [H4] (see Fig. 9 and the orange line in Fig. 11).

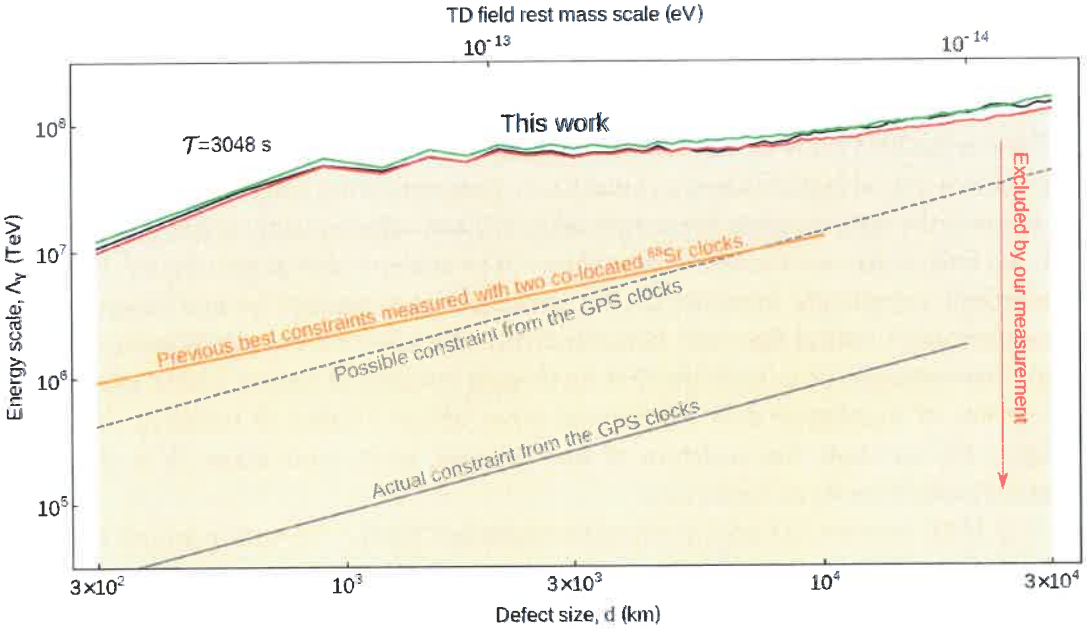

Fig. 11 Constraint (95% confidence levels, red line) on the strength of DM-SM coupling (i.e. the energy scale Λ_γ) determined with the global network of optical atomic clocks. The black and green lines are the direct fit and the 5% confidence level, respectively. The orange line is the previous best limit determined with two co-located ^{88}Sr clocks [H4], and the grey solid and dashed lines represents the actual and possible constraints, respectively, estimated from the GPS constellation's on-board clocks [Kalaydzhyan2017, Roberts2017].

In the work reported in Ref. [H5] we considered not only coupling of the hypothetical topological defects to electromagnetic filed, but also coupling of hypothetical oscillating massive scalar fields that would be manifested as harmonic perturbation of the fine-structure constant. Within this scenario, the clocks' readouts would be perturbed at frequency ω which is related to the scalar field mass as $m_\varphi = \hbar\omega/c^2$. In this analysis, aimed on searches for oscillating massive scalar fields, we used all our data spanning 114 days from all the laboratories. Here, we consider a linear coupling, whose strength is quantified by the dimensionless parameter

$$d_e = \frac{M_P c^2}{\sqrt{4\pi}\Lambda_{\gamma,1}},$$

where $M_P c^2 = 1.2 \times 10^{19}$ GeV is the Planck mass energy equivalent [Kalaydzhyan2017]. To search for the harmonic oscillation signatures we employed the procedure [Scargle1982] used in [Tilburg2015, Hees2016]. For every considered frequency we fit the normalized signals from all the clocks with a $R(t) = B + A(\omega)\cos(\omega t + \varphi)$ function, where B is a constant offset. We use the fitted amplitude, A, to determine the constraint on the coupling coefficient [H5]

$$d_e < \sqrt{\frac{A^2(\omega)\omega^2 c^2}{\rho_{DM} 8\pi G}},$$

where G is the Newton's constant. In Figure 12, we show the results of our analysis. The blue line corresponds to the direct fit and the red line is our actual constraint having statistical interpretation of 95 % confidence level [H5]. Our limit considerably exceeds, in a wide range of field masses, the previous spectroscopic limits determined with microwave atomic clocks [Hees2016] and dysprosium experiments [Tilburg2015] and is complementary to the completely independent equivalence principle tests [Williams2004, Schlamminger2008] and recent MICROSCOPE experiment [Bergé2018].

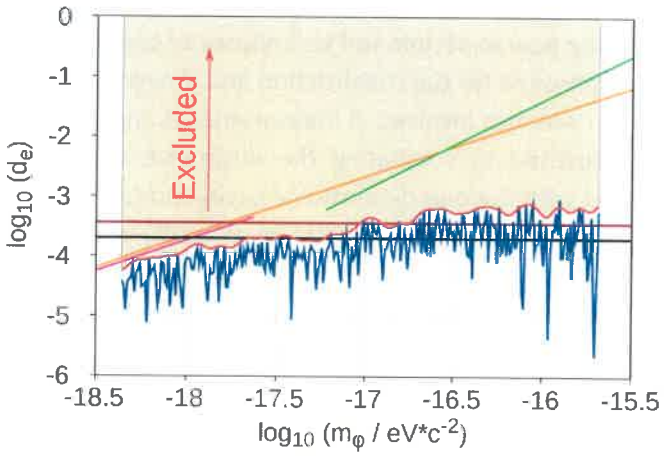

Fig. 12 Constraint on the coupling constant d_e (the 95% confidence level, red line). The blue line is the direct fit. The magenta and orange lines are the 95% confidence limits from Refs. [Hees2016] and [Tilburg2015], respectively. The green line is the limit obtained from the stability analysis of a single optical atomic clock [Kalaydzhyan2017]. The brown line represents the equivalence principle (EP) [Schlamminger2008, Williams2004]. The black line is the constraint obtained with the MICROSCOPE experiment [Bergé2018].

In Refs. [H4] and [H5] we developed new methods for searching for new hypothetical scalar fields that can explain the dark-matter problem. We studied their potential couplings with the electromagnetic field, that would be manifested as the perturbation of the fine-structure constant,

α. We demonstrated that a single optical atomic clock is sensitive to variations in α. We used this property to construct the first global network of optical atomic clock aimed on dark-matter searches. For the case of topological defects, our constraints considerably exceed the previous ones. For the case of oscillating massive scalar fields, our limits exceed the previous spectroscopic constraints and reach a similar level to other independent techniques.

1. Discussion of other scientific achievements:

1.1. Description of other achievements

Besides the achievements described in Sec. 4, after receiving the PhD degree I was involved in several other scientific projects:

- **Measurements and spectra analysis for the rovibronic transitions from highly excited vibrational (v = 11) states of H_2** [P1]. I was responsible for the analysis of Stark-perturbed shapes of the rovibronic lines in H_2 (the perturbations of the shapes were critical for the determination of the transitions' energies). This work constitute the first accurate validation of ab initio calculations of the H_2 structure for vibrationally highly excited states.

- ***Ab initio* calculations of the line-shape parameters for the He-perturbed H_2 molecule** [P2, P3, P4]. I was involved in potentials preparations, collisional calculations, results interpretation and line-shape effects analysis. In Ref. [P2] we report our first results for the Q(1) fundamental line and S(1) purely rotational line. In Ref. [P3] we extended the analysis for all the bands from v=0-0 to 0-5 for the Q branches. Finally, in [P4] we calculated the line-shape parameters for the same bands for the O and S branches. This project is important for providing the reference spectroscopic data for planetary atmosphere analysis and will be used for the construction of the first *ab initio* spectroscopic database.

- **Developing new experimental techniques of cavity-enhanced spectroscopy** [P5, P6]. I was responsible for the construction and development of the experimental setup. In Ref. [P5] I was also involved in measurements and data analysis. The work reported in [P5] is devoted to comparing the dispersive line shapes of molecular transition measured with the one-dimensional cavity mode dispersion spectroscopy (1D-CMDS) with the usual absorptive spectra from cavity ring-down spectroscopy (CRDS). The work reported in Ref. [P6] was focused on employing the 1D-CMDS method in the measurements of absolute molecular transition frequencies. This project [P5, P6] provides a new experimental technique that allows the apparatus systematic effect to be reduced considerably.

- **Developing the most widely used spectroscopic database HITRAN** [P7, P8]. I was responsible for introducing the new beyond-Voigt line-shape parametrization and construction of the comprehensive dataset for the self-perturbed H_2 spectra. In Ref. [P7] the HITRAN Application Programming Interface (HAPI) was introduced; this is a software that allows inexperienced users to benefit from advanced capabilities of the HITRAN database. Ref. [P8] describes the most recent, 2016, edition of the HITRAN database.

- **Developing methods for describing sophisticated line-shape effects in molecular spectra** [P9]. In this work we analyzed the dispersion corrections to the Gaussian profile. I was responsible for calculating the relativistic effects manifested in the shapes of molecular lines as well as for validating the derivations for the dispersion corrections. This analysis will be important in analysis of strong molecular lines measured with high signal-to-noise ratio (>10^5).

- **Line-shape analysis of Raman spectra of self- and He-perturbed purely rotational lines in D_2** [P10, P11]. I was responsible for line-shape analysis of the He-perturbed D_2 lines. In Ref. [P10] we tested our *ab initio* quantum scattering calculations the collisional on accurate Raman spectra. The work reported in Ref. [11] was focused on accurate determination of the energies of the purely rotational lines in D_2.

1.2. Other publications after receiving the PhD degree (not included in Sec. 4):

P 1. T. Madhu Trivikram, M. L. Niu, **P. Wcisło**, W. Ubachs, E. J. Salumbides, *Precision measurements and test of molecular theory in highly excited vibrational states of H_2 (v = 11)*, Appl. Phys. B 122, 294 (2016)

P 2. F. Thibault, **P. Wcisło**, R. Ciuryło, *A test of H_2-He potential energy surfaces*, Eur. Phys. J. D 70, 236 (2016)

P 3. F. Thibault, K. Patkowski, P. S. Żuchowski, H. Jóźwiak, R. Ciuryło, **P. Wcisło**, *Rovibrational line-shape parameters for H_2 in He and new H_2-He potential energy surface*, J. Quant. Spectrosc. Radiat. Transf. 202, 308 (2017)

P 4. H. Jóźwiak, F. Thibault, N. Stolarczyk, **P. Wcisło**, *Ab initio line-shape calculations for the S and O branches of H_2 perturbed by He*, J. Quant. Spectrosc. Radiat. Transf. 219, 313 (2018)

P 5. A. Cygan, S. Wójtewicz, M. Zaborowski, **P. Wcisło**, R. Guo, R. Ciuryło, D. Lisak, *One-dimensional cavity mode-dispersion spectroscopy for validation of CRDS technique*, Meas. Sci. Technol. 27, 045501 (2016)

P 6. A. Cygan, S. Wójtewicz, G. Kowzan, M. Zaborowski, **P. Wcisło**, J. Nawrocki, P. Krehlik, Ł. Śliwczyński, M. Lipiński, P. Masłowski, R. Ciuryło, D. Lisak, *Absolute molecular transition frequencies measured by three cavity-enhanced spectroscopy techniques*, J. Chem. Phys 144, 214202 (2016)

P 7. R. V. Kochanov, I. E. Gordon, L. S. Rothman, **P. Wcisło**, C. Hill, J. S. Wilzewski, *HITRAN Application Programming Interface (HAPI): A comprehensive approach to working with spectroscopic data*, J. Quant. Spectrosc. Radiat. Transf. 177, 15 (2016)

P 8. I.E. Gordon, L.S. Rothman, ..., **P. Wcisło**, S. Yuh, E. J. Zak, *The HITRAN2016 molecular spectroscopic database*, J. Quant. Spectrosc. Radiat. Transf. 203, 3 (2017)

P 9. S. Wójtewicz, **P. Wcisło**, D. Lisak, R. Ciuryło, *Dispersion corrections to the Gaussian profile describing the Doppler broadening of spectral lines*, Phys. Rev. A 93, 042512 (2016)

P 10. R. Z. Martínez, D. Bermejo, F. Thibault, **P. Wcisło**, *Testing the ab initio quantum-scattering calculations for the D_2–He benchmark system with stimulated Raman spectroscopy*, J. Raman Spectrosc. 49, 1339 (2018)

P 11. R. Z. Martínez, D. Bermejo, **P. Wcisło**, F. Thibault, *Accurate wavenumber measurements for the $S_0(0)$, $S_0(1)$ and $S_0(2)$ pure rotational Raman lines of D_2*, J. Raman Spectrosc. (2018), doi: 10.1002/jrs.5499

Bibliography

[Bergé2018] J. Bergé, P. Brax, G.Métris, M. Pernot-Borràs, P. Touboul, J.-P. Uzan, Phys. Rev. Lett. 120, 141101 (2018)

[Bober2015] M. Bober, P. Morzyński, A. Cygan, et al., Measurement Science and Technology 26, 075201 (2015)

[Calonico2015] D. Calonico, M. Inguscio, F. Levi, Europhys. Lett. 110, 1 (2015)

[Campargue2012] A. Campargue, S. Kassi, K. Pachucki, J. Komasa, Phys. Chem. Chem. Phys. 14, 802 (2012)

[Cheng2012] C.-F. Cheng, Y. R. Sun, H. Pan, J. Wang, A.-W. Liu, A. Campargue, S.-M. Hu, Phys. Rev. A 85, 024501 (2012).

[Cygan2015] A. Cygan, P. Wcisło, S. Wójtewicz, P. Masłowski, J.T. Hodges, R. Ciuryło, D. Lisak, Opt. Express 23, 14472 (2015)

[Cygan2016] A. Cygan, S. Wójtewicz, G. Kowzan, M. Zaborowski, P. Wcisło, J. Nawrocki, P. Krehlik, Ł. Śliwczyński, M. Lipiński, P. Masłowski, R. Ciuryło, D. Lisak, J. Chem. Phys. 144, 214202 (2016)

[Czachorowski2018] P. Czachorowski, M. Puchalski, J. Komasa, K. Pachucki, Phys. Rev. A (in press)

[Derevianko2014] A. Derevianko, M. Pospelov, Nat. Phys. 10, 933 (2014)

[Diddams2000] S. A. Diddams, D. J. Jones, J. Ye, S. T. Cundiff, J. L. Hall, J. K. Ranka, R. S. Windeler, R. Holzwarth, T. Udem, and T. W. Hänsch, Phys. Rev. Lett. 84, 5102 (2000)

[Drever1983] R. W. P. Drever, J. L. Hall, F. V. Kowalski, J. Hough, G. M. Ford, A. J. Munley, H. Ward, Appl. Phys. B 31, 97 (1983)

[Ghysels2017] M. Ghysels, Q. Liu, A. J. Fleisher, J. T. Hodges, Appl. Phys. B 123, 124 (2017)

[Gordon1954] J. P. Gordon, H. J. Zeiger, C. H. Townes, Phys. Rev. 95, 282 (1954)

[Gordon1955] J. P. Gordon, H. J. Zeiger, C. H. Townes, Phys. Rev. 99, 1264 (1955)

[Gordon2017] I.E. Gordon, L.S. Rothman, ..., P. Wcisło, S. Yuh, E. J. Zak, J. Quant. Spectrosc. Radiat. Transf. 203, 3 (2017)

[Gupta2007] M. Gupta, T. Owano, D. S. Baer, A. O'Keefe, Chem. Phys. Lett. 441, 204 (2007)

[Hachisu2015] H. Hachisu, T. Ido, Jpn. J. Appl. Phys. 54, 112401 (2015)

[Hachisu2018] H. Hachisu, F. Nakagawa, Y. Hanado, T. Ido, Scientific Reports 8, 4243 (2018)

[Hees2016] A. Hees, J. Guéna, M. Abgrall, S. Bize, P.Wolf, Phys. Rev. Lett. 117, 061301 (2016)

[Hinde2008] R. J. Hinde, J. Chem. Phys. 128, 154308 (2008)

[Hinkley2013] N. Hinkley, J. A. Sherman, N. B. Phillips, et al., Science 341, 1215 (2013)

[Hutson1994] J. M. Hutson, S. Green, Molscat computer code, version 14. MOLSCAT computer code, version 14, distributed by Collaborative Computational Project No 6 of the UK Science and Engineering Research Council (1994)

[Jóźwiak2018] H. Jóźwiak, F. Thibault, N. Stolarczyk, P. Wcisło, J. Quant. Spectrosc. Radiat. Transf. 219, 313 (2018)

[Kalaydzhyan2017] T. Kalaydzhyan, N. Yu, Phys. Rev. D 96, 075007 (2017)

[Kassi2012] S. Kassi, A. Campargue, K. Pachucki, J. Komasa, J. Chem. Phys. 136, 184309 (2012)

[Kassi2014] S. Kassi, A. Campargue, J. Mol. Spectrosc. 300, 55 (2014)

[Komasa2011] J. Komasa, K. Piszczatowski, G. Łach, M. Przybytek, B. Jeziorski, K. Pachucki, J. Chem. Theory Comput. 7, 3105 (2011)

[Lin2015] H. Lin, Z. D. Reed, V. T. Sironneau, and J. T. Hodges, J. Quant. Spectrosc. Radiat. Transfer 161, 11 (2015)

[Lodewyck2016] J. Lodewyck, S. Bilicki, E. Bookjans, et al., Metrologia 53, 1123 (2016)

[Ludlow2015] A. D. Ludlow, M. M. Boyd, J. Ye, E. Peik, P. O. Schmidt, Rev. Mod. Phys. 87, 637 (2015)

[Miller2005] C.E. Miller, L.R. Brown, R.A. Toth, D.C. Benner, V.M. Devi, C. R. Phys. 6, 876 (2005)
[Monchick1986] L. Monchick, L. W. Hunter, J. Chem. Phys. 85, 713 (1986)
[Mondelain2016] D. Mondelain, S. Kassi, T. Sala, D. Romanini, D. Gatti, A. Campargue, J. Mol. Spectrosc. 326, 5 (2016)
[Morville2005] J. Morville, S. Kassi, M. Chenevier, D. Romanini, Appl. Phys. B 80, 1027 (2005)
[Morzyński2015] P. Morzyński, M. Bober, D. Bartoszek-Bober, et al., Scientific Reports 5, 17495 (2015)
[Pine1999] A. S. Pine, J. Quant. Spectrosc. Radiat. Transfer 62, 397 (1999)
[Polyansky2015] O. L. Polyansky, K. Bielska, M. Ghysels, L. Lodi, N. F. Zobov, J. T. Hodges, and J. Tennyson, Phys. Rev. Lett. 114, 243001 (2015)
[Roberts2017] B. M. Roberts, G. Blewitt, C. Dailey, M. Murphy, M. Pospelov, A. Rollings, J. Sherman, W. Williams, A. Derevianko, Nature Communications 8, 1195 (2017)
[Salumbides2013] E. Salumbides, J. Koelemeij, J. Komasa, K. Pachucki, K. Eikema, W. Ubachs, Phys. Rev. D 87, 112008 (2013)
[Salumbides2015] E. J. Salumbides, A. N. Schellekens, B. Gato-Rivera, W. Ubachs, New. J. Phys. 17, 033015 (2015)
[Scargle1982] J. D. Scargle, Astrophys. J. 263, 835 (1982)
[Schaefer1992] J. Schaefer, L. Monchick, Astron. Astrophys. 265, 859 (1992)
[Schioppo2016] M. Schioppo, R. C. Brown, W. F. McGrew, et al., Nature Photonics 11, 48 (2016)
[Schlamminger2008] S. Schlamminger, K.-Y. Choi, T. A. Wagner, J. H. Gundlach, E. G. Adelberger, Phys. Rev. Lett. 100, 041101 (2008)
[Smith1989] W.H. Smith, C.P. Conner, J. Simon, W.V. Schempp, W. Macy, Icarus 81, 429 (1989)
[Tan2014] Y. Tan, J. Wang, C.F. Cheng, X.Q. Zhao, A.W. Liu, S.M. Hu, J. Mol. Spectrosc. 300, 60 (2014)
[Targat2013] R. Le Targat, L. Lorini, Y. Le Coq, et al., Nature communications 4, 2109 (2013)
[Tilburg2015] K. Van Tilburg, N. Leefer, L. Bougas, D. Budker, Phys. Rev. Lett. 115, 011802 (2015)
[Tran2013] H. Tran, N.H. Ngo, J.-M. Hartmann, J. Quant. Spectrosc. Radiat. Transf. 129, 199 (2013)
[Ubachs2016] W. Ubachs, J. Koelemeij, K. Eikema, E. Salumbides, J. Mol. Spectrosc. 320, 1 (2016)
[Udem1999] T. Udem, J. Reichert, R. Holzwarth, and T. W. Hänsch, Opt. Lett. 24, 881 (1999)
[Vilenkin1985] A. Vilenkin, Phys. Rep. 121, 263–315 (1985)
[Wcisło2014] P. Wcisło, H. Tran, S. Kassi, A. Campargue, F. Thibault, R. Ciuryło, J. Chem. Phys. 141, 074301 (2014)
[Wcisło2018] P. Wcisło, F. Thibault, M. Zaborowski, S. Wójtewicz, A. Cygan, G. Kowzan, P. Masłowski, J. Komasa, M. Puchalski, K. Pachucki, R. Ciuryło, D. Lisak, J. Quant. Spectrosc. Radiat. Transf. 213, 41 (2018)
[Williams2004] J. G. Williams, S. G. Turyshev, D. H. Boggs, Phys. Rev. Lett. 93, 261101 (2004)